Probing coalescence of light nuclei via femtoscopy and azimuthal anisotropies

Yoshini Bailung [1,*] Sudhir Pandurang Rode [2,†] Neha Shah [3,‡] and Ankhi Roy [1,§]

[1]*Department of Physics, Indian Institute of Technology Indore, Simrol, Indore 453552, Madhya Pradesh, India*

[2]*Veksler and Baldin Laboratory of High Energy Physics, Joint Institute for Nuclear Research, Dubna 141980, Moscow region, Russia*

[3]*Department of Physics, Indian Institute of Technology Patna, Bihta, Patna 801106, Bihar, India*

(Received 6 July 2024; revised 21 October 2024; accepted 9 January 2025; published 22 January 2025)

The production mechanism of light nuclei in heavy-ion collisions is vital to understanding the intricate details of nucleon-nucleon interactions. The coalescence of nucleons is a well-known mechanism that attempts to explain the production mechanism of these light clusters. This work investigates the formation mechanism of these nucleon clusters with a combination of coalescence and femtoscopy of nucleons and nuclei. It is achieved by appending a coalescence and correlation afterburner (CRAB) to the SMASH transport model. To have a proper view of the anisotropy of light nuclei clusters, a mean-field approach to SMASH is applied. The anisotropic coefficients of various light nuclei clusters are calculated and compared to experimental measurements. To incorporate hydrodynamics into the picture, the anisotropic measurements are completed in a hybrid SMASH+vHLLE mode. In both approaches, the femtoscopy of nucleons and light nuclei is performed, reported with CRAB, and compared to the latest experimental measurements. An insight into cluster formation time is drawn by extracting the emission source size with the Lednický-Lyuboshits model.

DOI: 10.1103/PhysRevC.111.014911

I. INTRODUCTION

The light nuclei production is believed to be sensitive to the baryon density fluctuations and can be utilized to probe the quantum chromodynamics (QCD) phase transition [1–4]. However, their production mechanism in heavy-ion collisions is not completely understood, despite various theoretical attempts made by an ensemble formalism via statistical hadronization, from nucleons' coalescence or stochastic processes [5–15]. Existing and upcoming experimental measurements of light nuclei can provide a vast testing ground for these models in search of the nature of such low-energy QCD interactions. Moreover, due to its bound nature, light nuclei states are an ideal probe for performing two-particle correlations and femtoscopy. Particle femtoscopy in heavy-ion collisions provides insight into particle emission's space-time geometry and their interactions [16–18]. Although femtoscopy for various hadrons has been measured, there is less exploration in the light nuclei regime. The ALICE collaboration first moved by looking into the p-d system and opening avenues to explore the emission of a few nucleon clusters [19–21]. Understanding the interaction of these many-nucleon systems can assist in the realization of the intricacies of nucleon-nucleon interactions, as well as the equation of state (EoS) of neutron stars. Theoretical predictions have provided the possibility of having three (p-d) and even four (d-d, p-t, p-^{3}He) nucleon-bound states that could be very well observed in heavy-ion collisions [22–28]. Recent efforts have been made by HADES [29] and STAR [30,31] collaborations on femtoscopic measurements of these states, providing an opportunity to understand their production mechanisms. In general, physicists pursue light nuclei production through nucleon coalescence, statistical transport reactions, or through the treatment of statistical hadronization given by the thermal model.

In principle, the few-nucleon cluster production can be explored by combining femtoscopy and coalescence. Recently, the STAR collaboration carried out such measurements in Au + Au collisions at $\sqrt{s_{NN}} = 3$ GeV for p-d and d-d states, followed by a transport model calculation with SMASH [30,32]. The deuterons from coalescence have shown an excellent ability to describe the experimental measurements. The findings of this study by STAR provide a hint at an inclination towards coalescence as a primary production mechanism of light nuclei. The emission source of the nucleon/nuclei pairs from the femtoscopic correlations shows a decreasing trend with the centrality in Au + Au collisions [30]. This is due to the source sizes being nontrivially affected by the colliding matters' expansion time, radially and longitudinally. The measurement of emission space-time geometry of particles can assist in drawing a clearer description of the collective nature of expansion. This is of particular interest to understanding anisotropic flow in noncentral heavy-ion collisions. The convolution between these two aspects of light nuclei production brings together a cohesive point of discussion about their production mechanism. Microscopic transport models such as UrQMD [33], AMPT [34], and more recent SMASH [32] are developed with one of many goals to interpret the generated anisotropies in

*Contact author: yoshini.bailung.1@gmail.com
†Contact author: sudhirrode11@gmail.com
‡Contact author: nehashah@iitp.ac.in
§Contact author: ankhi@iiti.ac.in

heavy-ion collisions. Non-central heavy-ion collisions lead to azimuthally asymmetric emission of particles, the distribution of which can be decomposed into a Fourier expansion in the particles' azimuthal angle (ϕ). Each Fourier harmonic constitutes a flow component, such as directed flow $v_1 = \langle \cos \phi \rangle$ and elliptic flow $v_2 = \langle \cos 2\phi \rangle$ corresponding to first and second harmonics, respectively [35,36].

Experimental evidence suggests that protons' elliptic flow coefficient is below zero at center-of-mass energies around and below 3 GeV [37]. Depending on the time scale of expansion in low energy collisions, the expanding matter can be blocked by the spectators in the reaction plane [38]. Subsequently, this leads to a "squeeze-out" effect if the blockage time from the spectators is more, forcing the emission out-of-plane [39,40]. This "effect" is arguably connected to a softening or hardening of the EoS, which the models exploit to explain the experimental measurements [41–44]. Fluid dynamical treatment with a 'soft' EoS fails to explain the negative elliptic flow. Here, the importance of mean-field interactions could be drawn out, which, in addition to the EoS, is an established approach to explain the flow of protons at low energies [40,45–48]. Many transport models can achieve this by parametrizing the Skyrme mean-field potential between the nucleons based on the "stiffness" of the EoS. Calculations with SMASH and UrQMD at low energies have reported success in reproducing experimental data from HADES and STAR of light nuclei flow with the application of a hard EoS [49,50].

In this work, we simulate Au + Au collisions at $\sqrt{s_{NN}} = 3$ GeV using the SMASH simulation package [32]. Our choice of beam energy is influenced by a couple of reasons, the first being the availability of the experimental measurements of light nuclei observables at this beam energy by the STAR collaboration [1,30]. Moreover, this beam energy falls into the region where new measurements from upcoming experiments such as compressed baryonic matter (CBM) at FAIR [51] and multipurpose detector (MPD) at NICA [52] are foreseen. We test our "*in situ*" coalescence model on different cluster formation times. This transport model is also used to generate the phase-space information of the nucleons at different 'nonstandard' freeze-out times. We refer to it as the last collision time of the nucleons. For closure, we employ a hard EoS mean field parametrization of the Skyrme potential in SMASH, as well as a hybrid treatment, where a fluid dynamical evolution is carried out with the vHLLE package [53,54]. We perform femtoscopic correlations on these clusters to validate the impact of different cluster formation times. The correlation afterburner (CRAB) model [55] is used to generate the momentum correlations of *p*-*d* and *d*-*d* pairs for varying centralities in Au + Au collisions at $\sqrt{s_{NN}} = 3$ GeV, which is compared to experimental results. Following the momentum correlations, we extract the source sizes of the light cluster systems by fitting the Lednický Lyuboshits (LL) model [56], with a Gaussian ansatz for the source. By varying the last collision times of the nucleons, we gain insight into the formation times from the emission sizes of these clusters. The last collision time is expected to be different for different nucleon bound states, which is tested out for *p*-*d* and *d*-*d* states. The results are also supplemented with the directed and elliptic flow of light clusters in midcentral Au + Au collisions.

The paper is arranged in the following manner. Section II is divided into Secs. II A and II B for the event generation methodology with SMASH and the coalescence model, respectively. Likewise, Sec. III has Secs. III A and III B dedicated to femtoscopy, explaining the source size estimation with the LL model and CRAB for the momentum correlations. Section IV presents the results, the correlation functions shown in Sec. IV A, and the anisotropic flow calculations in Sec. IV B. We conclude the paper by summarising the findings in Sec. V.

II. SMASH AND COALESCENCE

A. The SMASH transport model

The hadronic transport model SMASH, or "Simulating Many Accelerated Strongly interacting Hadrons" is a many-interaction model developed to extend the exploration of the QCD phase diagram to the low and intermediate beam energies [32]. In this regime, the prevailing degrees of freedom are that of hadrons, which usually do not require a hybrid treatment, unlike the dynamical transport models, which impose hybrid treatment of each stage of evolution of the collision. These dynamical models face challenges in the intermediate beam energies, which are of great interest to unlocking the attributes of the QCD phase diagram. However, SMASH has also been designed to operate in a hybrid mode, which allows it to be coupled with a relativistic hydrodynamic expansion. The hybrid SMASH is coupled to the vHLLE; a 3 + 1D viscous hydrodynamic model [53] that follows a well-known fluid expansion where the level of dilution is examined by a critical energy density cutoff. For the initial and final stages of the evolution, SMASH operates in a pure transport mode, following hydrodynamic expansion by the hadron sampler and a hadronic afterburner. Although at very low energies, a hydrodynamic treatment of the collision is not essential, it was an obvious choice in the light nuclei aspect to show a better description of the deuteron yields with the hydro turned on than a pure transport SMASH. It is to be noted that the default light nuclei treatment in SMASH is turned off. A well-detailed description of the modules can be found in Ref. [54].

For the mean-field approach, the interaction potentials in SMASH are parametrized to replicate the stiffness of EoS. The Skyrme and symmetry potential in SMASH is expressed as

$$U = U_{\rm sk} + U_{\rm sym}, \tag{1}$$

which, individually, are written as

$$U_{\rm sk} = A\left(\frac{\rho_B}{\rho_0}\right) + B\left(\frac{\rho_B}{\rho_0}\right)^{\tau}, \tag{2}$$

$$U_{\rm sym} = \pm 2 S_{\rm pot} \frac{\rho_{I_3}}{\rho_0}, \tag{3}$$

where ρ_B is the net baryon density, $S_{\rm pot}$ is the symmetry potential energy, $\rho_0 = 0.168\,{\rm fm}^{-3}$ is the nuclear ground state density, ρ_{I_3} is the density of the relative isospin projection. A hard EoS corresponds to a larger value of compressibility (K), which is tuned via the parameters A, B, and τ, the values for which are studied and used in Refs. [49,50,57]. In order to incorporate mean-field potentials, a test-particle formalism in SMASH is adopted, where each nucleon is represented by multiple test particles. This increases the phase space

density, reaching much higher multiplicities per event. Since the deuterons in this study are selected through a Wigner coalescence formalism, a different approach in coalescence between the Hard EoS and hydro SMASH is not needed. There will be a significant difference in the deuteron multiplicities between the two treatments, however it does not alter the observables that are used for this study.

B. The coalescence afterburner

With the phase-space information of the nucleons, a coalescence approach is applied to produce nuclei out of closely placed nucleons. This work takes a Wigner coalescence approach, where the nuclei wave function is expressed as a Wigner probability density [58]. Coalescence is achieved by checking the level of overlap between the phase space of the nucleons and the nuclei's Wigner probability. The position of the nucleon at the earlier time is propagated to the one at the later time. It is to be noted that the neighboring hadrons may cause finite-size effects during coalescence. However, their effect on our results is checked and is found to be a negligible fraction. The invariant yields for deuteron and triton/helium-3 can be expressed in the form

$$\begin{aligned}\frac{d^3N_{d(t/^3\mathrm{He})}}{dp^3_{d(t/^3\mathrm{He})}} &= \mathcal{S}_{d(t/^3\mathrm{He})}\int d^3\mathbf{r}_{d(t/^3\mathrm{He})}d^3\mathbf{r}(\mathbf{r}')d^3\mathbf{q}(\mathbf{q}')\\ &\times \mathcal{D}(\mathbf{r}(\mathbf{r}'),\mathbf{q}(\mathbf{q}'))W_{pn(p/n-np)}\\ &\times\left(\frac{\mathbf{p}_{d(t/^3\mathrm{He})}}{2}\pm\mathbf{q}(\mathbf{q}'),\mathbf{r}_{d(t/^3\mathrm{He})}\pm\frac{\mathbf{r}(\mathbf{r}')}{2}\right),\end{aligned} \tag{4}$$

respectively, where $\mathbf{r}_{d(t/^3\mathrm{He})}$, $\mathbf{p}_{d(t/^3\mathrm{He})}$, and $\mathbf{r}(\mathbf{r}')$, $\mathbf{q}(\mathbf{q}')$ are the cluster spatio-momenta and $\mathcal{S}_{d(t/^3\mathrm{He})}$ is the statistical spin-isospin averaging factor, $W_{pn(p/n-np)}$ is the nucleon pair selection probability term, and $\mathcal{D}$ is the Wigner probability density defined as

$$\mathcal{D}(\mathbf{r},\mathbf{q}) = \int d^3\xi e^{-i\mathbf{q}\cdot\xi}\varphi\left(\mathbf{r}+\frac{\xi}{2}\right)\varphi^*\left(\mathbf{r}-\frac{\xi}{2}\right). \tag{5}$$

The Wigner density can be derived from the light-nuclei structure, expressed by its quantum mechanical wave function, and can be related to the source function of the two and three-nucleon clusters. The deuteron wave function is approximated to be a single Gaussian function $\varphi(r) = \frac{1}{(\pi\sigma_d^2)^{3/4}}e^{-\frac{r^2}{2\sigma_d^2}}$ with root mean square (rms) charge radius $\sigma_d = 2.14$ fm[59]; consequently with the Wigner probability density becoming

$$\mathcal{D}(\mathbf{r},\mathbf{q}) = 8e^{-\frac{\mathbf{r}^2}{\sigma_d^2}-\mathbf{q}^2\sigma_d^2}. \tag{6}$$

In order to avoid any oversimplification from a Gaussian deuteron wavefunction while studying the quantum features via correlation functions, the calculations are extended to a realistic treatment of the deuteron. A double Gaussian form which is parametrized to the Hulthen wave function of the deuteron is chosen in this case [58], expressed as

$$\varphi(r) = \frac{1}{\pi^{3/4}}\left[\frac{\Delta^{1/2}}{\sigma_{d_1}^{3/2}}e^{-\frac{r^2}{2\sigma_{d_1}^2}} + \iota\frac{(1-\Delta)^{1/2}}{\sigma_{d_2}^{3/2}}e^{-\frac{r^2}{2\sigma_{d_2}^2}}\right], \tag{7}$$

where the parameters $\Delta = 0.247$, $\sigma_{d_1} = 5.343\,\mathrm{fm}^{-1}$, and $\sigma_{d_2} = 1.81\,\mathrm{fm}^{-1}$ are extracted by fitting Eq. (7) to the Hulthen wave function [60–62]. The Wigner density takes the form

$$\mathcal{D}(\mathbf{r},\mathbf{q}) = 8\left[\Delta e^{-\frac{\mathbf{r}^2}{\sigma_{d_1}^2}-\mathbf{q}^2\sigma_{d_1}^2} + (1-\Delta)e^{-\frac{\mathbf{r}^2}{\sigma_{d_2}^2}-\mathbf{q}^2\sigma_{d_2}^2}\right]. \tag{8}$$

For the three-nucleon clusters (t, ^{3}He), the Wigner probability is written as

$$\mathcal{D}(\mathbf{r},\mathbf{q},\mathbf{r}',\mathbf{q}') = 8^2 e^{-\frac{\mathbf{r}^2}{\sigma_{t/^3\mathrm{He}}^2}-\mathbf{q}^2\sigma_{t/^3\mathrm{He}}^2}e^{-\frac{\mathbf{r}'^2}{\sigma_{t/^3\mathrm{He}}^2}-\mathbf{q}'^2\sigma_{t/^3\mathrm{He}}^2}, \tag{9}$$

where $\sigma_t = 1.75$ fm, and $\sigma_{^3\mathrm{He}} = 1.96$ fm, are the charge rms radius of the triton and helium-3, respectively [59].

III. FEMTOSCOPY AND CRAB

A. Femtoscopy of light nuclei

Femtoscopy is performed via two-particle momentum correlations of like or unlike particle pairs, which gives the space-time picture of their emission from the interaction region [16–18]. Experimentally, the correlation function for a two-nucleon system can be obtained by taking the relative momentum (q^*) in the pair-rest frame of the nucleons. It can be defined as

$$C(q^*) = \frac{1}{\mathcal{N}}\frac{A(q^*)}{B(q^*)}, \tag{10}$$

where $A(q^*)$ and $B(q^*)$ are the two-nucleon correlation distributions in the same and mixed event, respectively, and $\mathcal{N}$ is a normalizing constant. The same distribution, in theory, can be expressed as a convolution of the source function $S(\mathbf{r})$ corresponding to the emission system and the wave function or the Bethe-Salpeter amplitude (Ψ) of the two-nucleon system given by

$$C(q^*) = \int d^3rS(\mathbf{r}) \mid \Psi(\mathbf{r},q^*) \mid^2 . \tag{11}$$

For identical pairs, the source function can be assumed to be a Gaussian of source radius r_0, to yield the correlation function of correlation strength λ as described below:

$$C(q^*) = 1 + \lambda e^{-q^{*2}r_0^2}. \tag{12}$$

In this study, however, we use the LL model [56,63], which is more exhaustive to Eq. (12) that considers final state interactions (FSIs) in the form of Coulomb and strong interactions, and quantum statistical fluctuations between the nucleons. The full correlation function for identical pairs can be defined as

$$\begin{aligned}C(q^*) = 1 + \lambda\Bigg(e^{-q^{*2}r_0^2} + \frac{1}{2}\Bigg(\left|\frac{f_c^S(k^*)}{r_0}\right|^2 + \frac{4\mathrm{Re}f_c^S(k^*)}{\sqrt{\pi}r_0}\\ \times F_1(q^*r_0) - \frac{2\mathrm{Im}f_c^S(k^*)}{\sqrt{\pi}}F_2(q^*r_0)\Bigg)\Bigg).\end{aligned} \tag{13}$$

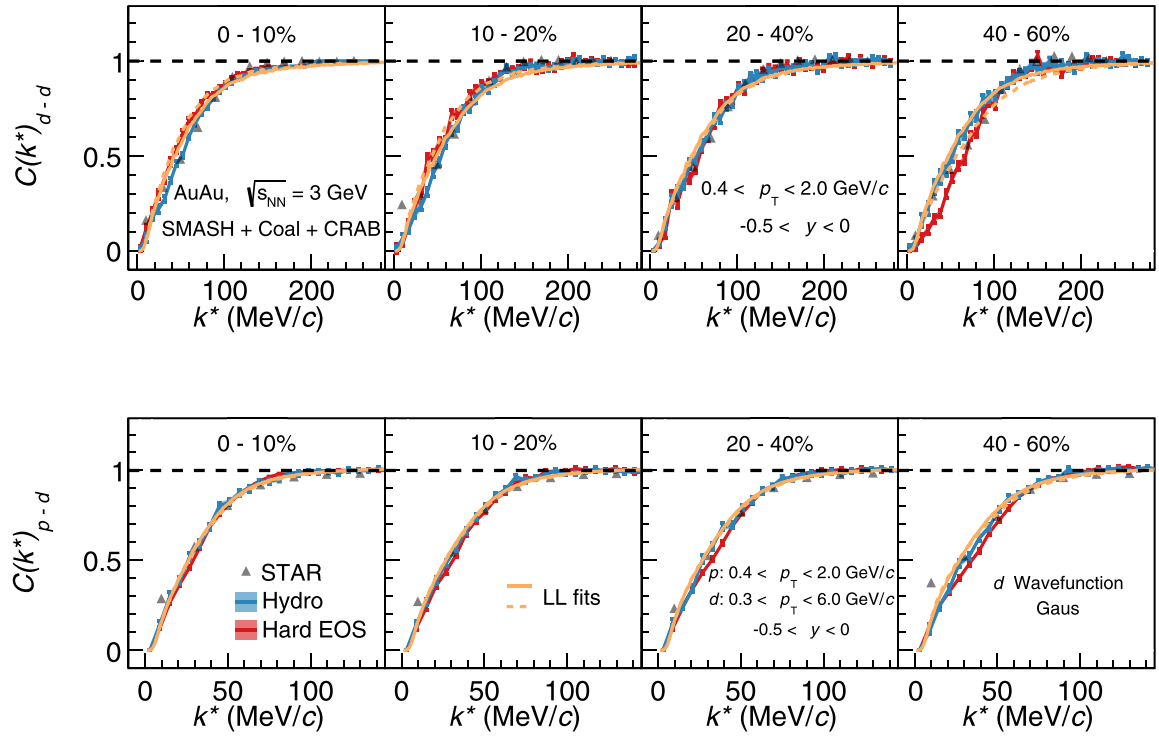

FIG. 1. Momentum correlation of p-d (bottom) and d-d (top) pairs with a Gaussian deuteron wave function in Au + Au collisions at $\sqrt{s_{NN}} = 3$ GeV in different centralities from SMASH + Coal + CRAB, compared to STAR preliminaries [30]. Predictions are presented for hydro and hard EoS SMASH fitted with the LL model shown in solid and dashed red lines, respectively.

For nonidentical pairs, the same expression can be approximated to

$$C(q^*) \approx 1 + \frac{1}{2}\left(\left|\frac{f_c^S(k^*)}{r_0}\right|^2 + \frac{4\mathrm{Re}f_c^S(k^*)}{\sqrt{\pi}r_0} \times F_1(q^*r_0) - \frac{2\mathrm{Im}f_c^S(k^*)}{\sqrt{\pi}}F_2(q^*r_0)\right). \quad (14)$$

$f_c^S(k^*)$ is the forward scattering amplitude with Coulomb interactions for a given total spin S, and functions $F_1(z) = \frac{1}{2}e^{-z^2}\int_0^z e^{x^2}dx$, and $F_2(z) = \frac{1}{z}(1 - e^{-z^2})$. The LL model has been extensively used to extract source sizes and interaction parameters in experimental femtoscopy studies for various particle systems. Light nucleon/nuclei correlations of the p-d and d-d kind have been studied by the STAR collaboration for Au + Au collisions at $\sqrt{s_{NN}} = 3$ GeV across different centralities [30]. This study will use the LL model to fit the nuclei correlation distributions obtained via CRAB, to which the light-nuclei states from the coalescence model will be fed. Although coalescence considers a finite-size formalism of the deuteron, an apriori "point-particle" assumption is taken for the usability of the LL model. Since the formation of the deuterons is taken very early in the hadronic evolution and closer to the particlization hypersurface, the size of the correlating species can be considered to be much less than the emission source deuteron is a finite-sized, making a fitting scenario for the LL model.

B. Correlation afterburner (CRAB)

To perform the momentum correlation of the nucleon/nuclei states, with the inclusion of quantum statistics and FSIs, a "correlation-afterburner" CRAB [55] is coupled to SMASH. To perform light nuclei femtoscopy, the coalescence model generates the input to CRAB, to carry out momentum correlations for $p-d$ and $d-d$ states. The working of CRAB is based on the correlation function defined as

$$C(p, q) = \frac{\int d^4x_1 d^4x_2 S_1(x_1, p_2) \cdot S_2(x_2, p_1)|\phi(q, r^*)|^2}{\int d^4x_1 S_1(x_1, p_1) \int d^4x_2 S_2(x_2, p_2)}, \quad (15)$$

where (x, p) is the phase space information of the nucleons/nuclei, $S_i(x, p)$ is the probability of emitting particle i at phase space (x_i, p_i), $p(q)$ are the total (relative) momentum, r^* is the relative position, and $\phi(q, r^*)$ is the overlap wave function of the pair; used to build the pair correlation functions. We compare the results to the experimental measurements with the correlations generated from the combination of SMASH, coalescence, and CRAB.

IV. RESULTS AND DISCUSSION

A. Correlation functions

Figures 1 and 2 show the predictions of momentum correlation functions from SMASH + Coal + CRAB of p-d and d-d pairs in different collision centralities, with Gaussian and double Gaussian treatments of the deuteron wave function, respectively. The LL model fits to the correlation functions are

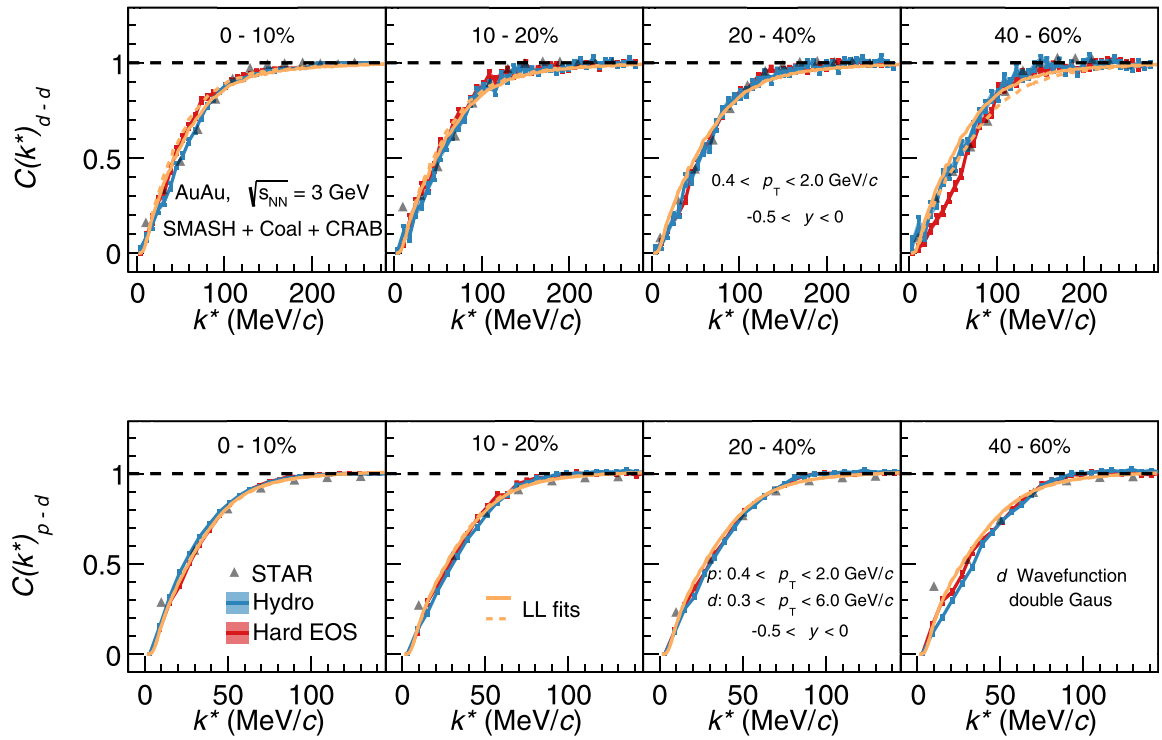

FIG. 2. Momentum correlation of p-d (bottom) and d-d (top) pairs with a double Gaussian deuteron wave function of the deuteron in Au + Au collisions at $\sqrt{s_{NN}} = 3$ GeV in different centralities from SMASH + Coal + CRAB, compared to STAR preliminaries [30]. Predictions are presented for hydro and hard EoS SMASH fitted with the LL model shown in solid and dashed red lines, respectively.

also included in the figures. SMASH is configured in two ways viz., with hydro and with a hard EoS. The correlation distributions are obtained from the CRAB afterburner, which takes in the nucleon (nuclei) phase-space from SMASH (SMASH + Coal). As CRAB is not designed for p-d correlations, the potential for p-d interactions is adapted from [25]. The correlations are tested on two cluster formation times 20 and 30 fm/c up to which SMASH hadronic cascade is evolved and at which point the coalescence of nucleon pairs is carried out. The p-d and d-d femtoscopy results presented in Figs. 1 and 2 are for cluster formation times 20 fm/c and 30 fm/c, respectively, for hydro and hard EoS SMASH. The results are compared to the preliminary measurements from STAR [30]. Except at 40–60 % centrality, where a deviation between the hydro and hard EoS is noticed, the results from both wavefunction treatments show excellent agreement with the data for p-d and d-d correlations. A closer look reveals that the hydro predictions are slightly better than the hard EoS selection, especially noticeable for d-d pairs at peripheral collisions.

To gain a more quantitative insight and compare the formation times, we extract the source sizes of the p-d and d-d pairs. The source sizes are extracted by fitting the LL model to the correlation distributions, assuming a Gaussian emission source. The fits are performed on the SMASH + Coal + CRAB results, as well as on the STAR preliminary measurements [30]. In Figs. 1 and 2, we report the fits to the SMASH + Coal + CRAB outputs across different centralities for p-d and d-d correlation functions from the two wave function treatments, for hydro and hard EoS configurations. The source sizes reported in Fig. 3 show a decreasing dependence with centrality for the STAR data. The p-d cluster source sizes are larger, lying between 3–3.5 fm, in contrast to 1.8–2 fm for the d-d system. The SMASH + Coal + CRAB results for p-d pairs are well reproduced at 20 fm/c for hydro, with a slight underestimation by the hard EoS. At 30 fm/c, the source sizes overestimate the data, showing deviations upto 30%. The results for d-d pairs also predict the decreasing trend of source sizes with centrality, affirmed by the experimental results. Here, the scale of disagreement between the cluster formation times is less compared to the p-d pairs. Hydro SMASH offers the closest description at 30 fm/c. The hard EoS show 10% overestimation for central collisions, with closer description at midcentral to peripheral collisions. At 20 fm/c, the source radii are slightly lower than 30 fm/c, except at 40–60 % for hydro.

Even with finely spaced cluster formation times, we see variation in the p-d and d-d correlations reflected in the emission source radii. Based on the agreement with the data, we report that a cluster time at 30 fm/c for the deuteron is closer to describing the emission of d-d pairs, whereas a shorter time between 20–30 fm/c is preferred for the proton and deuteron pairs for the p-d cluster. This noteworthy observation indicates the formation time of differently populated baryon clusters formed in these heavy-ion collisions. The single and double Gaussian wave function treatments within uncertainties showing negligible differences also affirm the robustness of the coalescence approach in capturing the momentum correlations of the light clusters.

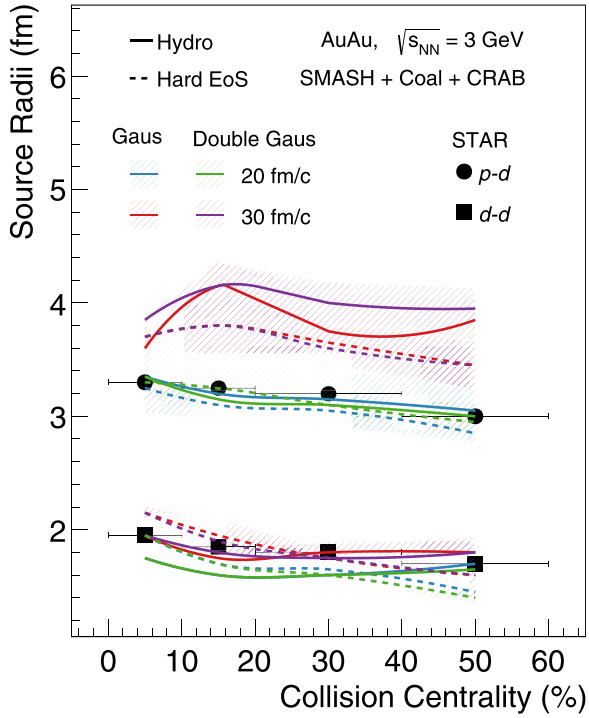

FIG. 3. Source radius extracted from LL fits to *p-d* and *d-d* correlation functions from STAR preliminaries [30], and from two cluster formation times in hydro (solid lines) and hard EoS (dashed lines) SMASH + Coal.

B. Anisotropic flow

Now, we focus on estimating the azimuthal anisotropies of light nuclei in 10–40 % central Au + Au collisions at $\sqrt{s_{NN}} = 3$ GeV. We estimate the directed (v_1) and elliptic flow (v_2) of deuterons, triton, and helium-3 and compare it with the extensive set of measurements performed by STAR collaboration [1]. Like the previous subsection, the flow coefficients are estimated for two variants of SMASH. The cluster's last collision time is taken from comparing the correlation functions from the previous subsection. However, we report that the flow calculations do not show a large sensitivity to the choice of the last collision time. In addition, the deuteron results are presented for the two variants of wave functions used in the study. The kinematic selections are kept the same as reported by the STAR measurements. We begin by studying the rapidity dependence of these flow coefficients, especially v_1, as it can reveal insights into the longitudinal dynamics of the collision. Figure 4 presents the dependence of v_1 and v_2 of light nuclei as a function of rapidity (y), in specific p_T regions ($0.8 < p_T < 2.0\,\mathrm{GeV}/c$ for deuteron and $1.2 < p_T < 3.0\,\mathrm{GeV}/c$ for triton/helium-3). Here, the coefficients of all species show considerable sensitivity to different SMASH modes, in particular, v_2. The hydro SMASH mode overestimates the measured v_2 of all light nuclei species by almost a factor of 2.

In addition to this and, more importantly, the SMASH + Coal + hydro variant fails to describe the negative values of v_2 (out-of-plane flow) at central rapidity intervals. It is worth noting that the hydro mode appears to reproduce the trend of

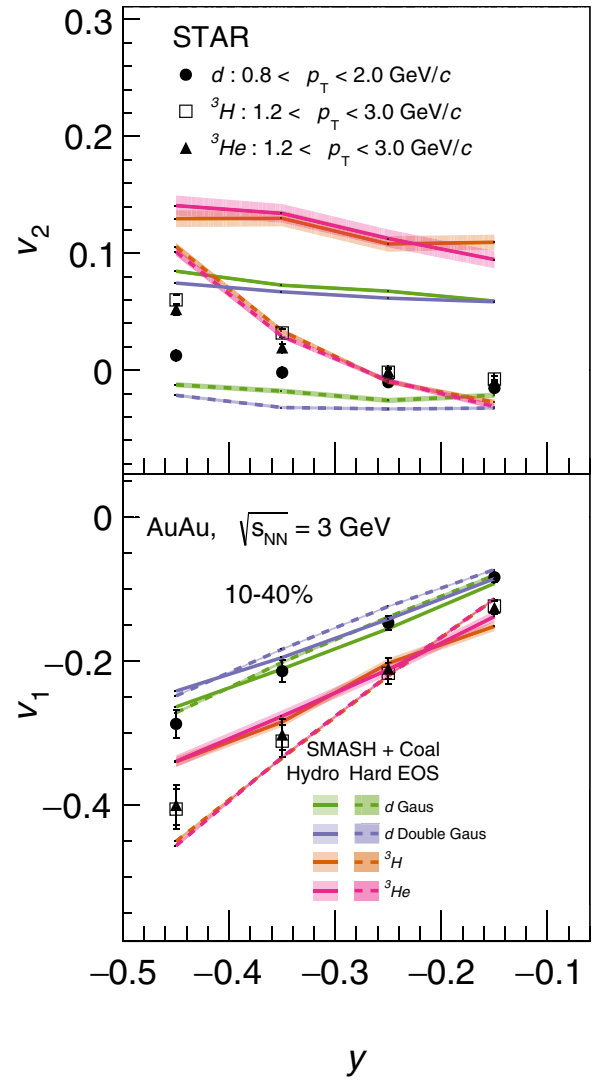

FIG. 4. Elliptic flow (v_2) and directed flow (v_1) of deuterons, tritons and helium-3 produced in noncentral Au + Au collisions as function of rapidity using SMASH + Coal. Results are compared to experimental measurements from STAR [1].

v_2. On the contrary, SMASH + Coal + hard EoS reproduce the negative values and reasonably describe the light nuclei v_2 measurement at central rapidity; however, they slightly underestimate the values at forward rapidities. This is possibly due to an effect of spectators or fragments from beam remnants that have an increasing rapidity dependence. The deuteron results with the double Gaussian wavefunction treatment show a slight underestimation of the v_2 in both hydro and hard EoS configurations. An account of mean-field contributions from hardening of the EoS seems to explain the 'squeeze-out' and out-of-plane emission of the deuteron, describing light nuclei v_2 at such low beam energy. In retrospect, the v_1 of light nuclei is qualitatively described by both modes of SMASH. Here, the double Gaussian configuration slightly overestimates the data than the single Gaussian treatment. Hard EoS provides a closer description of the rapidity dependence of deuteron v_1, as compared to hydro. This is a consequence of the

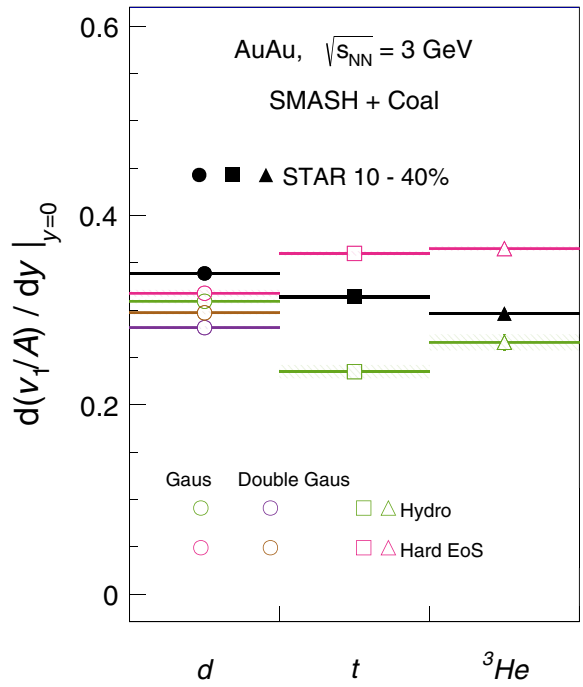

FIG. 5. dv_1/dy of deuterons, tritons and helium-3 produced in noncentral Au + Au collisions using SMASH + Coal compared to experimental measurements from STAR [1].

different phase space treatment in the two modes, leading to an effect from more low momenta deuterons from spectators. This observation is more apparent for triton and helium-3, where the hydro and Hard EoS modes under and overestimate towards increasing rapidity ($-0.4 < y < -0.3$), respectively. However, both hydro mode and hard EoS reproduce the mass ordering in both v_1 and v_2 as observed in experimental measurement.

The slope of directed flow (dv_1/dy) is an interesting observable for the investigation since it is sensitive to the underlying EoS as well as one of the candidates to provide insights about the dynamics of the QCD medium. As mentioned above, both modes of SMASH describe the v_1 slope; however, we have performed quantitative comparison with experimental measurements. In Fig. 5, we present this observable of light nuclei with hydro and hard EoS SMASH and compare it with STAR measurements [1]. The slope is estimated by fitting the v_1 within the rapidity window, $-0.5 < y < 0.0$, using a first-order polynomial scaled to the respective mass numbers. The slopes corresponding to the deuterons from single Gaussian Wigner coalescence, and hard EoS configuration are closer to the experimental results, showing about 6% deviation, while the hydro results show a larger deviation ∼9%. A systematic decrease in the slope upto 9% is noted for the deuterons with double Gaussian than the single Gaussian coalescence. On the other hand, the slopes for triton and helium deviate on either side of the data, creating a band with hard EoS and hydro with deviation up to ∼25%.

Moving forward, the transverse momentum dependence of directed flow coefficient (v_1) of d, t, and ^{3}He as a function of p_T in different rapidity intervals is shown in Fig. 6. Both SMASH modes, hard EoS, and hydro agree with the measurements across the whole p_T range from 1 to 3 GeV/c and rapidity intervals. The p_T dependence of elliptic flow coefficients (v_2) of light nuclei in different rapidity regions are shown in Fig. 7. The SMASH modes show deviations similar to the results in Fig. 4, with a positive and increasing with p_T v_2 for d, t, and ^{3}He with hydro turned on. However, the failure of hydro in reproducing the sign suggests that SMASH + Coal + hydro at a low center-of-mass energies may not be enough to describe the "squeeze-out" of colliding matter that eventually leads to a negative flow. The hard EoS reproduces this phenomenon well across p_T and rapidity region, asserting the importance of the mean-field approach. To check the robustness of the results, similar calculations of these flow coefficients were carried out using different last collision times for the clusters, and it was found that it did not change the message of our findings. For the specific case of the deuteron, the two wavefunction treatments do not show any discernible difference in the p_T dependent flow coefficient results.

In the literature [38] and [50], it has been argued that at low energies, neither soft nor hard EoS describe the v_1 and v_2 together convincingly. However, we have seen in our work that, unlike hard EoS, soft EoS failed to explain the rapidity and p_T dependence of both v_1 and v_2. Since different transport model approaches have various underlying degrees of freedom, different conclusions regarding mean-field interaction strengths can be drawn. It has already been seen that existing FOPI data [41] is very nicely explained by soft EoS [45], and approaches with a hard EoS over UrQMD shows agreement with the NA49 and HADES measurements [42,44,49]. Moreover, deuterons via transport interactions in SMASH have demonstrated the requirement of a hard EoS and asserts its importance in describing the HADES experimental results in Au + Au collisions at $E_{kin} = 1.23$ GeV [50].

V. CONCLUSIONS

In this article, we investigate the momentum correlation function of nucleons and light nuclei and gain insight into their production times and their sensitivity to the initial anisotropy in heavy-ion collisions. The SMASH transport model generates the nucleon phase space, passing through a coalescence afterburner to form the light nuclei states. SMASH is operated in two configurations: a hybrid configuration with a viscous hydrodynamics treatment and a mean-field configuration with a hard EoS.

The protons and deuterons from coalescence are used as input to the CRAB afterburner to generate the momentum correlations of p-d and d-d states. The deuteron states from Wigner coalescence are obtained with two treatments of the deuteron wave function; (i) a single Gaussian form and (ii) a double Gaussian form, which is parametrized to the Hulthen wave function of the deuteron. The correlation functions are obtained at different collision centralities compared to experimental measurements at STAR. The correlations are fitted with the LL model, assuming a Gaussian emission source. The emission source radius of the p-d, d-d states from the fits shows a decreasing trend with increasing centrality. The

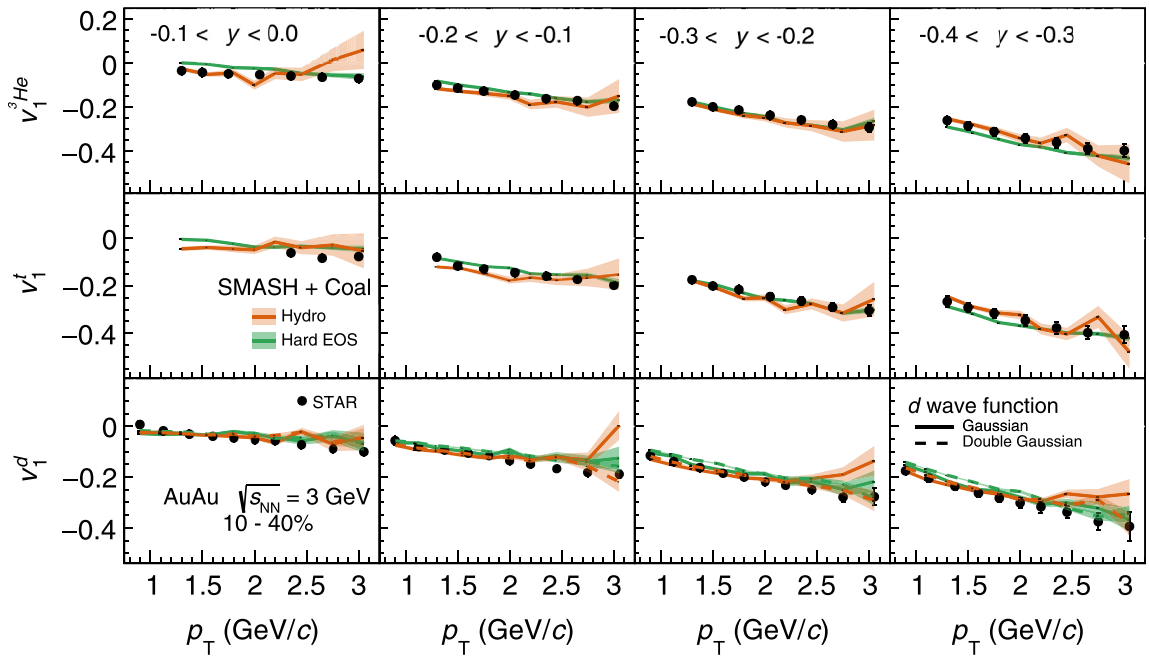

FIG. 6. Directed flow (v_1) as function of p_T of deuterons, tritons and helium-3 produced in noncentral Au + Au collisions using SMASH and their comparison with experimental measurements from STAR experiment [1].

results do not show any sensitivity to the underlying wave function used during coalescence. The excellent agreement of these predictions with the data asserts the importance of coalescence playing an important role in light nuclei formation. The calculations are verified by varying the cluster formation time of the nucleons/nuclei. We report that a difference of 10 fm/c is observed between the p-d cluster and the d-d cluster, the former being produced earlier. This is a testament to the sensitivity of formation times for different sources during the medium evolution.

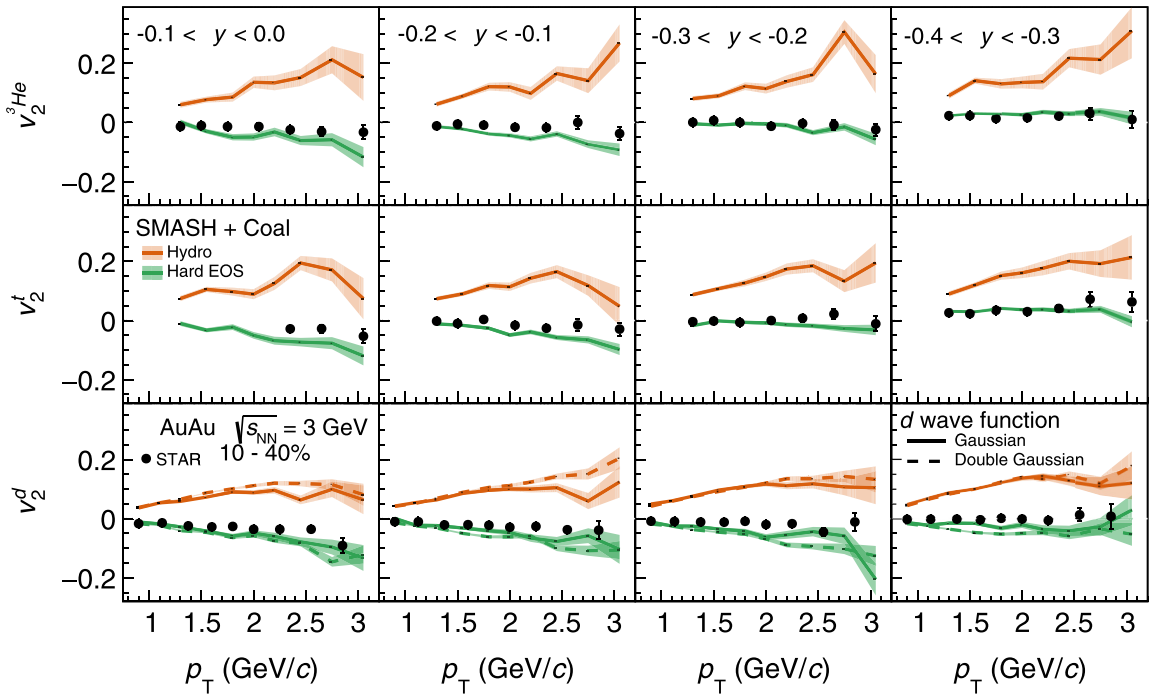

FIG. 7. Elliptic flow (v_2) as function of p_T of deuterons, tritons and helium-3 produced in noncentral Au + Au collisions using SMASH and their comparison with experimental measurements from STAR experiment [1].

To look into the influence of formation times on the collective expansion of the light clusters, we look at the directed and elliptic flow coefficients of the deuteron, triton, and helium-3 from coalescence for midcentral Au + Au collisions. In particular, we compare a mean-field potential approach to a hybrid approach of particle production in low-energy Au + Au collisions. Both treatments do not have noticeable differences for the directed flow of light nuclei but differ considerably for v_2. We report that the flow coefficients of the light nuclei are less sensitive to the last collision time, contrary to the observation made for the femtoscopic study. This observation provides the conclusion that momentum correlation measurements serve as a good observable to access formation times of the light clusters, as opposed to flow measurements. The results also allow us to conclude that a mean-field treatment with a hard EoS parametrization gives a precise description at low collision energies. We also reiterate that SMASH with soft EoS failed to describe rapidity and p_T dependence of both flow coefficients. Other studies involving deuteron production via transport processes with SMASH also strengthen this argument.

The findings shared in this analysis provide new avenues to extend and perform similar studies to other light and hypernuclei species (p-^{3}He, p-t, t-t, p-$_\Lambda{}^3$H). Femtoscopy studies of these states can provide more insight into the nucleon-nucleon interactions while estimating their formation times via coalescence. Moreover, the estimation of the emission source sizes scanned over a collision energy range would shed more light on the energy dependence and the formation time of these clusters. Such studies can be carried out once more data become available in the near future.

ACKNOWLEDGMENTS

Y.B. thanks all the members of the SMASH collaboration, Prof. S. Pratt for the CRAB package, and Prof. Lednický for providing us with the LL model. Y.B. is thankful to Swapnesh Khade for the fruitful discussions. This work uses computational facilities supported by the DST-FIST scheme via SERB Grant No. SR/FST/PSI-225/2016, by the Department of Science and Technology (DST), Government of India.

[1] M. S. Abdallah *et al.* (STAR Collaboration), Phys. Lett. B **827**, 136941 (2022).
[2] T. Anticic *et al.* (NA49 Collaboration), Phys. Rev. C **94**, 044906 (2016).
[3] K.-J. Sun, L.-W. Chen, C. M. Ko, and Z. Xu, Phys. Lett. B **774**, 103 (2017).
[4] N.-U. Bastian, P. Batyuk, D. Blaschke, P. Danielewicz, Y. B. Ivanov, I. Karpenko, G. Röpke, O. Rogachevsky, and H. H. Wolter, Eur. Phys. J. A **52**, 244 (2016).
[5] A. Andronic, P. Braun-Munzinger, J. Stachel, and H. Stocker, Phys. Lett. B **697**, 203 (2011).
[6] J. Cleymans, S. Kabana, I. Kraus, H. Oeschler, K. Redlich, and N. Sharma, Phys. Rev. C **84**, 054916 (2011).
[7] P. Hillmann, K. Käfer, J. Steinheimer, V. Vovchenko, and M. Bleicher, J. Phys. G **49**, 055107 (2022).
[8] J. Steinheimer, K. Gudima, A. Botvina, I. Mishustin, M. Bleicher, and H. Stocker, Phys. Lett. B **714**, 85 (2012).
[9] N. Shah, Y. G. Ma, J. H. Chen, and S. Zhang, Phys. Lett. B **754**, 6 (2016).
[10] W. Zhao, K. j. Sun, C. M. Ko, and X. Luo, Phys. Lett. B **820**, 136571 (2021).
[11] K.-J. Sun, C. M. Ko, and Z.-W. Lin, Phys. Rev. C **103**, 064909 (2021).
[12] S. Gläßel, V. Kireyeu, V. Voronyuk, J. Aichelin, C. Blume, E. Bratkovskaya, G. Coci, V. Kolesnikov, and M. Winn, Phys. Rev. C **105**, 014908 (2022).
[13] L. A. Dal and A. R. Raklev, Phys. Rev. D **91**, 123536 (2015); **92**, 069903(E) (2015); **92**, 089901(E) (2015).
[14] Y. Bailung, N. Shah, and A. Roy, Nucl. Phys. A **1037**, 122701 (2023).
[15] D. Everett *et al.* (JETSCAPE Collaboration), Phys. Rev. C **106**, 064901 (2022).
[16] M. A. Lisa, S. Pratt, R. Soltz, and U. Wiedemann, Annu. Rev. Nucl. Part. Sci. **55**, 357 (2005).
[17] L. Adamczyk *et al.* (STAR Collaboration), Phys. Rev. C **92**, 014904 (2015).
[18] S. Acharya *et al.* (ALICE Collaboration), Nature (London) **588**, 232 (2020); **590**, E13 (2021).
[19] B. Singh, PoS **EPS-HEP2021**, 391 (2022).
[20] H. Appelshäuser, Rev. Mex. Fis. Suppl. **3**, 4 (2022).
[21] S. Acharya *et al.* (ALICE Collaboration), Phys. Rev. X **14**, 031051 (2024).
[22] A. Kievsky, M. Viviani, and L. E. Marcucci, Phys. Rev. C **69**, 014002 (2004).
[23] K. Sekiguchi, Few Body Syst. **60**, 56 (2019).
[24] S. C. Pieper, V. R. Pandharipande, R. B. Wiringa, and J. Carlson, Phys. Rev. C **64**, 014001 (2001).
[25] B. K. Jennings, D. H. Boal, and J. C. Shillcock, Phys. Rev. C **33**, 1303 (1986).
[26] R. Kotte *et al.* (FOPI Collaboration), Eur. Phys. J. A **6**, 185 (1999).
[27] D. H. Boal, C. K. Gelbke, and B. K. Jennings, Rev. Mod. Phys. **62**, 553 (1990).
[28] R. Q. Wang, J. P. Lv, Y. H. Li, J. Song, and F. L. Shao, Chin. Phys. C **48**, 053112 (2024).
[29] M. Stefaniak, arXiv:2402.09280.
[30] K. Mi (STAR Collaboration), Acta Phys. Polon. Supp. **16**, 1-A91 (2023).
[31] D. Mallick (STAR Collaboration), Acta Phys. Polon. Supp. **16**, 1-A80 (2023).
[32] J. Weil *et al.* (SMASH Collaboration), Phys. Rev. C **94**, 054905 (2016).
[33] S. A. Bass, M. Belkacem, M. Bleicher, M. Brandstetter, L. Bravina, C. Ernst, L. Gerland, M. Hofmann, S. Hofmann, J. Konopka *et al.*, Prog. Part. Nucl. Phys. **41**, 255 (1998).
[34] Z. W. Lin, C. M. Ko, B. A. Li, B. Zhang, and S. Pal, Phys. Rev. C **72**, 064901 (2005).
[35] A. M. Poskanzer and S. A. Voloshin, Phys. Rev. C **58**, 1671 (1998).
[36] J. Adams *et al.* (STAR Collaboration), Phys. Rev. C **72**, 014904 (2005).

[37] C. Pinkenburg *et al.* (E895 Collaboration), Phys. Rev. Lett. **83**, 1295 (1999).
[38] P. Danielewicz, R. Lacey, and W. G. Lynch, Science **298**, 1592 (2002).
[39] P. Danielewicz, R. A. Lacey, P. B. Gossiaux, C. Pinkenburg, P. Chung, J. M. Alexander, and R. L. McGrath, Phys. Rev. Lett. **81**, 2438 (1998).
[40] Y. Nara and A. Ohnishi, Phys. Rev. C **105**, 014911 (2022).
[41] W. Reisdorf *et al.* (FOPI Collaboration), Nucl. Phys. A **876**, 1 (2012).
[42] H. Petersen, Q. Li, X. Zhu, and M. Bleicher, Phys. Rev. C **74**, 064908 (2006).
[43] V. P. Konchakovski, W. Cassing, Y. B. Ivanov, and V. D. Toneev, Phys. Rev. C **90**, 014903 (2014).
[44] P. Hillmann, J. Steinheimer, and M. Bleicher, J. Phys. G **45**, 085101 (2018).
[45] J. Aichelin, A. Rosenhauer, G. Peilert, H. Stoecker, and W. Greiner, Phys. Rev. Lett. **58**, 1926 (1987).
[46] M. Isse, A. Ohnishi, N. Otuka, P. K. Sahu, and Y. Nara, Phys. Rev. C **72**, 064908 (2005).
[47] A. Le Fèvre, Y. Leifels, C. Hartnack, and J. Aichelin, Phys. Rev. C **98**, 034901 (2018).
[48] Y. Nara, H. Niemi, J. Steinheimer, and H. Stöcker, Phys. Lett. B **769**, 543 (2017).
[49] P. Hillmann, J. Steinheimer, T. Reichert, V. Gaebel, M. Bleicher, S. Sombun, C. Herold, and A. Limphirat, J. Phys. G **47**, 055101 (2020).
[50] J. Mohs, M. Ege, H. Elfner, and M. Mayer, Phys. Rev. C **105**, 034906 (2022).
[51] D. Almaalol, M. Hippert, J. Noronha-Hostler, J. Noronha, E. Speranza, G. Basar, S. Bass, D. Cebra, V. Dexheimer, D. Keane *et al.*, arXiv:2209.05009.
[52] V. Golovatyuk, V. Kekelidze, V. Kolesnikov, O. Rogachevsky, and A. Sorin, Eur. Phys. J. A **52**, 212 (2016).
[53] I. Karpenko, P. Huovinen, and M. Bleicher, Comput. Phys. Commun. **185**, 3016 (2014).
[54] A. Schäfer *et al.* (SMASH Collaboration), Eur. Phys. J. A **58**, 230 (2022).
[55] S. Pratt, Correlation Afterburner [CRAB-3.0], https://web.pa.msu.edu/people/pratts/freecodes/crab/home.html.
[56] R. Lednicky and V. L. Lyuboshits, Yad. Fiz. **35**, 1316 (1981).
[57] H. Kruse, B. V. Jacak, and H. Stöcker, Phys. Rev. Lett. **54**, 289 (1985).
[58] Y. Bailung, N. Shah, and A. Roy, Phys. Rev. C **109**, 044908 (2024).
[59] F. Bellini and A. P. Kalweit, Phys. Rev. C **99**, 054905 (2019).
[60] M. Kachelrieß, S. Ostapchenko, and J. Tjemsland, Eur. Phys. J. A **56**, 4 (2020).
[61] M. Kachelrieß, S. Ostapchenko, and J. Tjemsland, Eur. Phys. J. A **57**, 167 (2021).
[62] M. Kachelrieß, S. Ostapchenko, and J. Tjemsland, Phys. Rev. C **108**, 024903 (2023).
[63] K. Morita, S. Gongyo, T. Hatsuda, T. Hyodo, Y. Kamiya, and A. Ohnishi, Phys. Rev. C **101**, 015201 (2020).